J Arid Land (2021) 13(12): 1260–1273
https://doi.org/10.1007/s40333-021-0026-0

Science Press Springer-Verlag

Mass balance of saline lakes considering inflow loads of rivers and groundwater: the case of Lake Issyk-Kul, Central Asia

Kei SAITOH[1*], Rysbek SATYLKANOV[2], Kenji OKUBO[3]

[1] Beppu Geothermal Research Laboratory, Institute for Geothermal Sciences, Graduate School of Science, Kyoto University, Oita 8740903, Japan;
[2] Tien Shan High Mountain Research Center, Institute of Water Problem and Hydropower of National Academy of Sciences of Kyrgyz Republic, Bishkek 720033, Kyrgyzstan;
[3] Graduate School of Environmental and Life Science, Okayama University, Okayama 7008530, Japan

Abstract: This study aimed to elucidate the influence of inflow water on the salinity concentration process of a saline lake and the mass balance of Lake Issyk-Kul, a tectonic saltwater lake in Kyrgyzstan. Based on the survey results and meteorological data from 2012 to 2015, we analyzed the dissolved chemical composition loads due to water inflow. Then, we discussed the relationship between the increase in salinity and water inflow into the lake. Through the water quality analysis data, we used the tank model to estimate the river inflow and analyze the loads by the L-Q curve. The groundwater loads were then estimated from the average annual increase in salinity of the lake over a period of 30 a. The results suggest that Lake Issyk-Kul was temporarily freshened between about AD 1500 and 1800 when an outflowing river existed, and thereafter, it became a closed lake in AD 1800 and continued to remain a saline lake until present. The chemical components that cause salinization are supplied from the rivers and groundwater in the catchment area, and when they flow into the lake, Ca^{2+}, HCO_3^- and Mg^{2+} precipitate as $CaCO_3$ and $MgCO_3$. These compounds were confirmed to have been left on the lakeshore as evaporite. The model analysis showed that 1.67 mg/L of Ca^{2+} and Mg^{2+} supplied from rivers and groundwater are precipitated as evaporite and in other forms per year. On the other hand, salinity continues to remain in the lake water at a rate of 27.5 mg/L per year. These are the main causes of increased salinity in Lake Issyk-Kul. Since Na^+ and Cl^- are considered to be derived from geothermal water, they will continue to flow in regardless of the effects of human activities. Therefore, as long as these components are accumulated in Lake Issyk-Kul as a closed lake, the salinity will continue to increase in the future.

Keywords: groundwater; geothermal water; mass balance; salinity; saline lake; L-Q curve

Citation: Kei SAITOH, Rysbek SATYLKANOV, Kenji OKUBO. 2021. Mass balance of saline lakes considering inflow loads of rivers and groundwater: the case of Lake Issyk-Kul, Central Asia. Journal of Arid Land, 13(12): 1260–1273. https://doi.org/10.1007/s40333-021-0026-0

1 Introduction

Most of saline lakes are located in arid regions, which are closed spaces and sensitive to anthropogenic activities and climate change. To understand the water cycle system, it is very important to understand the geophysical and chemical mechanisms of saline lakes from the

*Corresponding author: Kei SAITOH (E-mail: saitoh.k@bep.vgs.kyoto-u.ac.jp)
Received 2021-08-26; revised 2021-12-13; accepted 2021-12-17

viewpoint of global environmental conservation. Global climate warming is reported to be lowering the water levels of inland lakes around the world (Gross, 2017). In the Dead Sea, the water level has decreased by 1 m/a between 1996 and 2001 (Lensky et al., 2005). In addition, Lake Urmia, Great Salt Lake, Walker Lake, Aral Sea Owes Lake, etc., have shown significant decreases in water volume over the past 140 a (Wurtsbaugh et al., 2017). The decrease in the water level of Great Salt Lake is said to be caused not only by global warming but also by increased use of water by human activities (Shope and Angeroth, 2015). To address this issue, researchers have widely conducted internationally on water mass balance (e.g., Meng, 2019; Alifujiang, 2021). On the other hand, changes in salinity due to lowering of the lake level have also attracted attention in recent years (Benduhn and Renard, 2004; Chen, 2019). Changes in the salinity of lakes have a significant impact on the ecological environment and are therefore an important environmental issue. In order to solve these problems, it is necessary to quantitatively understand the unique water quality characteristics of lakes and their interrelationships with rivers and groundwater.

It is known that water quality composition of saline lakes varies from lake to lake, for example, Crater Lake in Uganda has a Na-HCO_3 type composition and Stony Lake in Canada has a Mg-SO_4 type composition (Livingston, 1963). The water quality classification of salt lakes can be explained by the large and small relationships between Ca^{2+} and HCO_3^- in the inflowing water (Mochizuki et al., 2018). For example, in the case of a Na-Cl-CO_3 type saline lake, if the concentration of HCO_3^- in the inflowing water is higher than that of Ca^{2+}, the amount of Ca^{2+} will decrease because it will flocculate and precipitate as $CaCO_3$. On the other hand, the supply of HCO_3^- by the influent water will continue. As salinity enrichment progresses, the water quality of the lake becomes of the Na-Cl-CO_3 type as the water is enriched in Na^+, Cl^- and HCO_3^- (Eugster and Hardie, 1978). Therefore, to clarify the process of water quality formation in saline lakes, it is important to understand the quality of inflow water.

To elucidate the material balance, it is first necessary to estimate the influent loads. Loads are calculated by multiplying the flow rate for each river by the dissolved chemical composition. The load-flow curve (i.e., L-Q curve) is an empirical formula for load (L) and flow (Q), and after deriving the L-Q curve, the loads can be calculated from the flow value. The L-Q curve is mainly used to estimate the impact of anthropogenic pollution (Yokota et al., 2013; Miyazako et al., 2014; Sugai et al., 2016; Le et al., 2020), and few examples of its use in elucidating the process of water quality formation in saline lakes are reported. However, quantitative understanding of the chemical constituents flowing into saline lakes will lead to future predictions on the increase and decrease of salinity and to an understanding of the mechanism of water quality formation in saline lakes.

Lake Issyk-Kul, the target area of this study, is a saline lake in Kyrgyzstan. It has experienced an increasing trend in salinity since the field observations made in 1986, and the salinity is still increasing (Kawabata et al., 2014; Saitoh and Kodera, 2019). The lake level showed a downward trend since 1929, but again an increasing trend since 1999 (Fukushima, 2006; Romanovsky et al., 2013; Salamat et al., 2015). The relationship between water level and salinity fluctuations is irregular and the cause of the increase in salinity cannot be clarified from the water balance alone. The water quality of the lake in the early 2000s was of the Na-SO_4, Cl type, but now, it is of the Na-Cl, SO_4 type and the water quality is changing (Karmanchuk, 2002; Kawabata et al., 2014). Saitoh (2019) and Saitoh and Kodera (2019) believe that these changes are closely related to the quality of the inflowing water, and they surveyed the catchment river and groundwater between 2012 and 2015. These studies have revealed the current status of water environment in the region by analyzing the dissolved chemical components in the rivers and groundwater around Lake Issyk Kul. The geographic understanding of water quality characteristics of the rivers and groundwater in the region has been achieved, but the interaction of rivers and groundwater with the lake has not been studied.

As mentioned above, it is important to focus the discussion on the water quality formation

mechanism and the water cycle system of saline lakes in order to understand the changes in water quality of saline lakes due to climate change and human activities. Therefore, in this study, in order to understand the mass balance mechanism of saline lakes, we estimated the inflow water loads in the catchment area of the lake based on the results of survey conducted in Lake Issyk-Kul during the period 2012–2015. The impact of the inflow on the lake water quality and the change in salinity from the past to the future were also discussed.

2 Materials and methods

2.1 Study area

Lake Issyk-Kul is a tectonic lake located in Kyrgyzstan between north and south mountain ranges at an altitude of over 3000 m a.s.l. (42°25′N, 77°20′E; Fig. 1). The water composition is of the Na-Cl, SO_4 type, with a salinity of 0.6% and a pH of 9.0, indicating its high alkalinity (Savvaitova and Petr, 1992; Tsigelnaya, 1995; Kawabata et al., 2014). The area of the lake is in an oval extending from east to west with an area of 6236 km^2. The maximum depth of the lake is 668 m with an average depth of 278 m, a water storage capacity of 1738 km^3 and a surface elevation of 1607 m from the data of 2012 (International Lake Environment Committee, 2003; Romanovsky et al., 2013).

Field observations and water quality analysis results reported by Saitoh (2019) and Saitoh and Kodera (2019) were used in this study. The survey was conducted in the summer during the period 2012–2015. Na^+, K^+, Ca^{2+}, Mg^{2+}, Cl^-, HCO_3^-, SO_4^{2-} and NO_3^- were analyzed by the absolute calibration curve method using ion chromatography (Shimadzu IC10ADVP, Kyoto, Japan). A 10-mL sample was prepared and filtered through a polyethersulfone membrane syringe filter with a pore size of 0.45 μm before analysis. Then, the sample was diluted with pure water so that the concentration of each component would be within the concentration range of the calibration curve, referring to the electrical conductivity measured in the field. HCO_3^- was analyzed by quantitative calculation from the amount of inorganic carbon using a total organic carbon (TOC) analyzer (Shimadzu TOC-VCSH, Kyoto, Japan). For the TOC analyzer, it is possible to prepare a sample of about 10 mL and analyze it directly. The analytical accuracy of these methods is 0.1 mg/L or less and the coefficient of variation (CV) is within 10%.

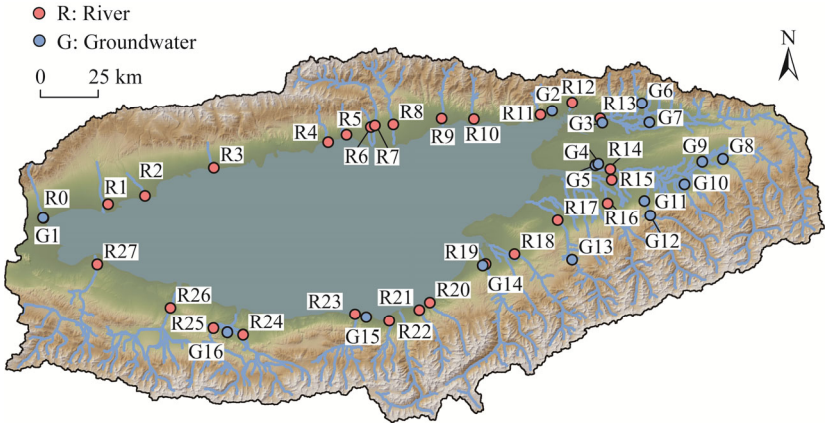

Fig. 1 Study area of Lake Issyk-Kul and survey sites of water samples during the period 2012–2015 (Adapted and modified from Saitoh (2019), and Saitoh and Kodera (2019))

The sampling points for the water quality data used were 15 river sites in 2012 (late August to early September); 15 river sites and 2 spring sites (17 sites in total) in 2013 (late August); 16 river sites and 1 spring site (17 sites in total) in 2014 (late August); and 23 river sites and 16 groundwater sites (39 sites in total) in 2015 (late August) (Fig. 1). The date and time of collection

and data for each site are shown in Table S1. River water quality data were used for almost all estuarine areas from where water flowed into the lake. Groundwater was collected from the pumped wells and springs in the periphery and eastern part of the lake (G1–G11, G14–G16). Water was also collected from hot springs managed by a recreational facility in the southeastern part of the lake (G12 and G13). All the samples were collected in summer. In Lake Issyk-Kul, summer is a time of heavy precipitation and high river inflow (Romanovsky et al., 2013). Normally, water samples should be taken in all months, but if there are no events such as typhoons or heavy rains, the water quality is not expected to change significantly.

2.2 Runoff model

The tank model devised by Sugawara (1972) was convinced by the researchers for a long-term analysis over centuries. A recent application of the model by Le et al. (2020) demonstrated the loading procedures through flux paths of surface and subsurface discharge from multiple watersheds into a deep lake. An overview of the model in this study is shown in Figure 2, where the routine is based on water depth in each story of the tanks arranged in series. Tank water will seep into the lower tank over time, or flow out through the side holes set at a certain height. Only the roof tank additionally receives both rainfall and evaporation. The lateral runoff from tanks does not start until the water level in each tank reaches the height of the side hole, but infiltrates into the lower tanks for any positive depth. The side discharges from each tank are the surface discharge at the top, intermediate discharge at the middle and groundwater discharge at the bottom. In this study, the tanks were set up in four stages (Fig. 2). In addition to surface discharge, intermediate discharge and groundwater discharge, we considered deep groundwater discharge, including the water from hot springs. This deep groundwater was not included in the river discharge, but was assumed to flow directly into the lake.

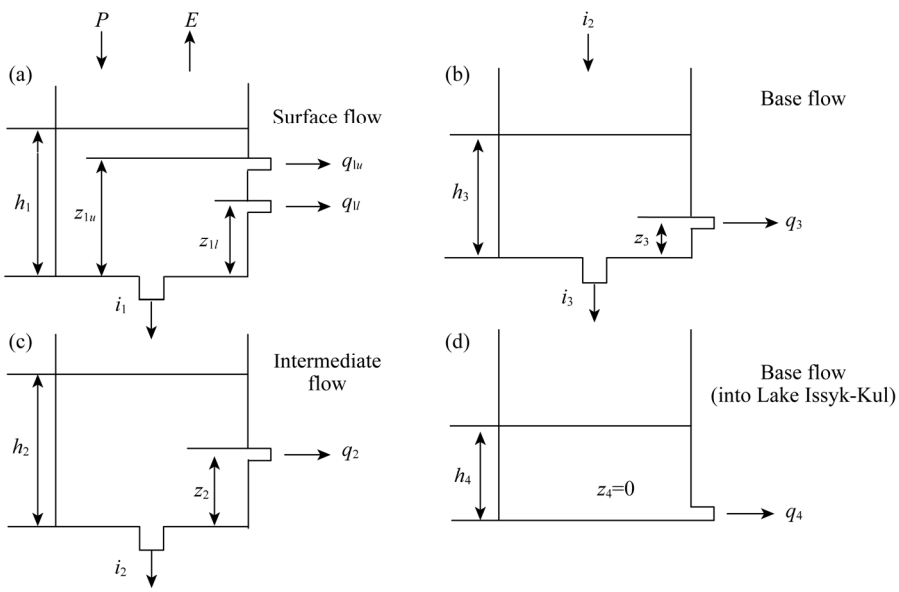

Fig. 2 Overview of the tank model. *P*, precipitation; *E*, evaporation; h_i is the water depth in the tank (storage height; mm); z_i is the height to the side hole (mm); i_i and q_i are the leachate and discharge (mm/d), respectively.

The water budgets are described as following equations:

$$dH / dt = \sum (P - E + Q / A)i, \tag{1}$$

$$dh_1/dt = P - E - i_{i-1} - q_i - i_i, \tag{2}$$

$$q_{1b} = \alpha_{1b}\left(h_1 - z_{1b}\right);\ i = \beta_1 h_1, \tag{3}$$

$$dh_i/dt = i_{i-1} - q_i - i_i, \tag{4}$$

$$q_i = \alpha_i \left(h_i - z_i \right);\ i_i = \beta_i h_i, \tag{5}$$

$$Q = Q_r + Q_g, \tag{6}$$

$$Q_r = \sum_{j=1}^{3} \left(q_j A / \Delta t \right);\ Q_g = q_4 A / \Delta t, \tag{7}$$

where H is the water level of the lake (m); P and E are the precipitation and evaporation (mm/d), respectively; Q is the discharge (m^3/s); A is the drainage area of each watershed (km^2); h_i is the water depth in the tank (storage height; mm); i_i and q_i are the leachate and discharge (mm/d), respectively; α_i and β_i are the constants that specify runoff and infiltration rates proportional to the relative height to the runoff outlet and the tank depth, respectively; z_i is the height to the side hole (mm); Q_r is the river discharge (m^3/s); Q_g is the groundwater discharge (m^3/s). The temporal integrals (dt and Δt) were done using a time increment of 1 d (86,400 s).

We calculated evaporation rate based on Dalton's model (Korzukhin et al., 2011) as follows:

$$E = \rho C_E U (e_s - e_a) / P, \tag{8}$$

where E is the evaporation rate (mm/d); ρ is the air density (1.2 kg/m^3); C_E is the bulk coefficient; U is the daily averaged wind speed (m/s); e_s and e_α are the saturated and actual water vapor pressures (hPa), respectively; and P is the atmospheric pressure (hPa). Since it is difficult to include wind speed neglecting wind direction, we considered the coefficient $C_E U/P$ as an average constant and adjusted it to obtain the optimal ratio of the total evaporation to precipitation (Le et al., 2020), i.e., r_E as shown in the following equation:

$$r_E = \sum E / \sum P;\ r_G = \sum Q_g / \sum Q_r. \tag{9}$$

This equation allows us to adjust fraction of evaporation (r_E) and groundwater (r_G) for the lake water variability of Lake Issyk-Kul (Romanovsky, 2013).

2.3 L-Q curve

In this study, following Amano and Kazama (2012) and Le et al. (2020), the relationship among gravimetric C_i (g/m^3), dissolved chemical constituent loads L_i (g/s), and discharge Q (m^3/s) is shown in Equation 10.

$$C_i = k_i Q^m;\ L_i = k_i Q^{m+1}, \tag{10}$$

where k_i and m are the coefficient and power exponent, respectively with units relating to the dimensional discharge.

A normalized discharge, $\hat{Q}$ avoids dimensional issues above and fixes the k_i unit as of concentration, as the dimensional intercept on the regime curve at $\hat{Q} = 1$, where Q_1 is a unit discharge taken as 1 m^3/s.

$$\hat{Q} = \left(Q_r + Q_g \right) / Q_1. \tag{11}$$

While a virtual discharge, $\tilde{Q}$ is used to estimate a chemical flux,

$$\tilde{Q} = Q_r + \gamma Q_g, \tag{12}$$

where γ represents the extra loads due to groundwater discharge at the bottom of the lake (m^3/s) and the higher the value, the greater the loads attributed to groundwater discharge. When the exponent $p=m+1$ is close to unity for a constant concentration ($m=0$) in Equation 10, the loads (L_g, m^3/s) due to groundwater discharge can be calculated as follows:

$$L_g = k \gamma Q_g. \tag{13}$$

3 Results

3.1 Construction of the tank model and L-Q curve

In the tank model, water balance and its composition can be obtained from Equations 1–7. We

established the tank model inflow estimates using data from 1 January, 2005 to 31 December, 2015. For estimating the flow rate, precipitation data from three meteorological observatories were obtained from the World Meteorological Organization. These data were used because Lake Issyk-Kul is vast and the precipitation varies from region to region. Therefore, the watershed was also divided into three regions and the flow rate was estimated for each region. The three meteorological observatories are Ka-dzhi-Say, Cholpon-Ata and Karakol, located in the southern, northern and eastern parts of the lake, respectively. The western part of the lake was not considered because this region lacks observatories and only traces of the lake's outflow rivers and few inflow rivers are present. The parameters used in the tank model are shown in Table S2.

To estimate the hourly or annual flow rate and loads strictly, calibration using actual measured data is necessary, but it is very difficult to obtain the flow observation data. Therefore, we refer to the water level fluctuation of the lake as an alternative data. In this study, the water balance data of Savvaitova and Petr (1992), Tsigelnaya (1995) and Romanovsky et al. (2013) were used for verification. Water balance data include precipitation, evaporation, river inflow, groundwater inflow and lake-level fluctuation. The data show an annual precipitation of 280 mm, a river inflow of 208 mm, a groundwater inflow of 330 mm, an evaporation of 814 mm and an annual lake-level fluctuation of 110 mm/a. According to the actual measurements, precipitation is invariant data; hence, Equation 9 was used to fit the lake-level fluctuation.

The L-Q curve was then examined using the above tank model and water quality analysis data from 2012 to 2015. The dates and times of the data used are shown in Table S1. The relationship between L and Q of river water in the study area is shown in Figure 3a. From this result, L was calculated from Q, and it was proved that exponent p in Equation 10 is close to 1. The relationship between L and Q when the exponent p is set to 1 and the equation for calculating the loads based on river inflow obtained from the regression is shown in Figure 3b. The river flow around Lake Issyk-Kul is generally high from June to August. Since the samples were collected mainly in August, the water quality was considered to correspond to that of a period of relatively high river flow during the year.

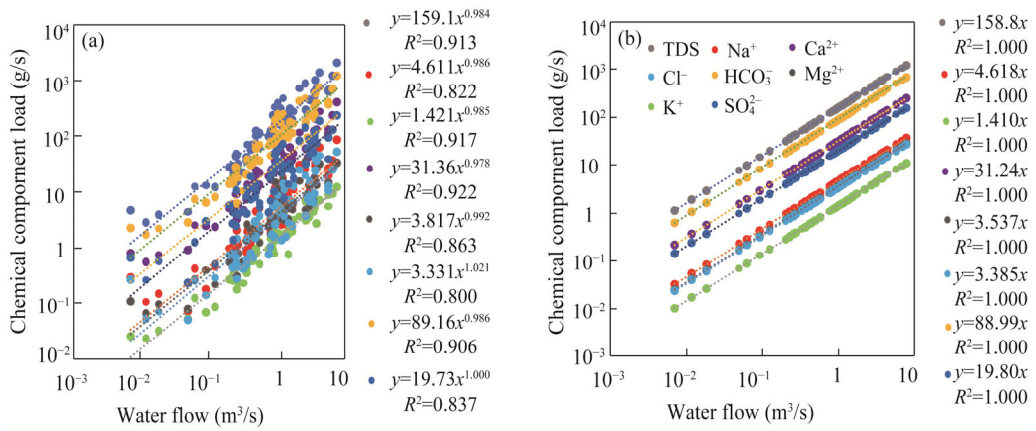

Fig. 3 Correlation between loads and flows in three (Ka-dzhi-Say, Cholpon-Ata and Karakol) catchment rivers. Original correlation (a) when exponent p is 1 (b).

3.2 Relationships of increased salinity with inflow river and groundwater loads in Lake Issyk-Kul

In this study, we proved that exponent p in Equation 10 is as close to 1 as possible. This makes it possible to dimensionally determine the groundwater loads using Equation 13. For setting γ, the average change in salinity per year at Lake Issyk-Kul during 1986–2015 was used as a reference. The change in lake salinity over time is summarized in Figure 4. According to this figure, the annual increase in each dissolved chemical constituent for about 30 a by actual measurement is

0.300 mEq/L for Na^++K^+, −0.010 mEq/L for Ca^{2+}, −0.020 mEq/L for Mg^{2+}, 0.220 mEq/L for Cl^-, 0.003 mEq/L for HCO_3^- and 0.080 mEq/L for SO_4^{2-}. The number of years required for this increase to reach the salinity of the lake in 2015 was 245 a for Na^+, 18,680 a for K^+, 225 a for Cl^-, 30 a for HCO_3^- and 530 a for SO_4^{2-}. The time required differs with the components because of different outputs such as precipitation as minerals and absorption by plants. Among different components, Na^+ and Cl^- are stable dissolved substances and tend to remain in the lake water. Therefore, we adjusted γ based on 235 a, which is the average of required years for Na^+ and Cl^-. With regard to the relationship between the number of years and historical background of the lake, Lake Issyk-Kul is said to have been an open lake with a temporary outflow river during AD 1500–1800 (Fig. 5; Rickets et al., 2001; Narama, 2012). If we assume that the lake was desalinated once between AD 1500 and 1800, this value of 235 a is reasonable.

The actual input k and γ are listed in Table 1. The higher the value of γ, the greater the loads due to groundwater discharge. This suggests that most of chemical components in the lake water are supplied by groundwater. Among the components, Na^+ and Cl^- are more strongly influenced by groundwater. On the other hand, the γ values of Ca^{2+} and HCO_3^- are lower than those of other chemical components, suggesting that most of them are supplied by rivers.

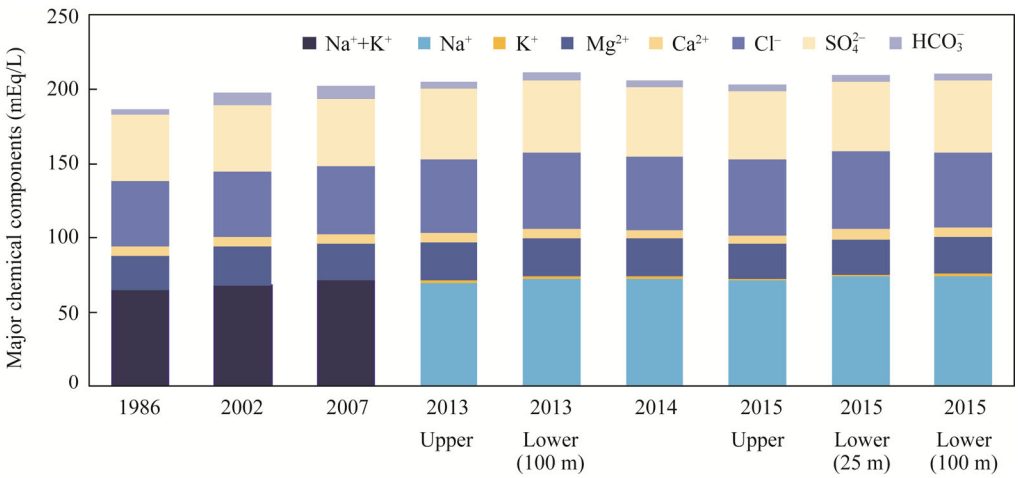

Fig. 4 Variation in the major chemical components in Lake Issyk-Kul over time (Adapted and modified from Saitoh (2019)). HCO_3^- from 1986 to 2007 is based on conversion from alkalinity. Upper indicates the surface layer of the lake, and lower indicates the deep water layer of the lake.

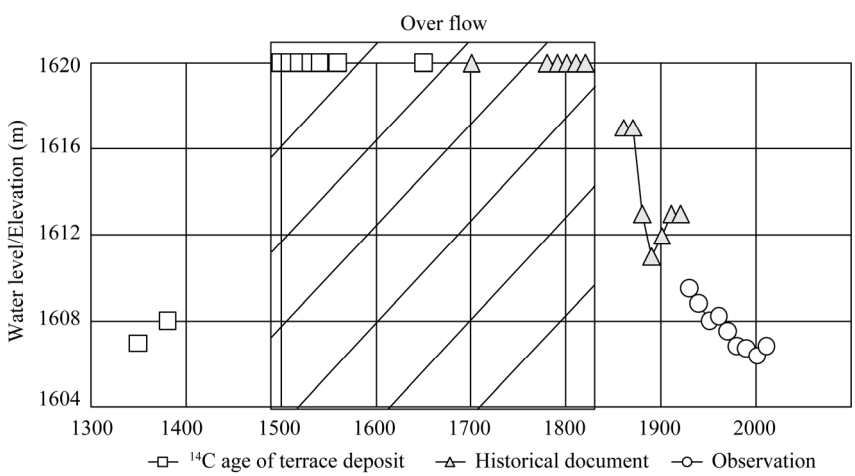

Fig. 5 Changes of water level in Lake Issyk-Kul over the past 700 a (Adapted and modified from Romanovsky et al. (2002); Fukushima (2006); Narama (2012); Romanovsky et al. (2013))

Table 1 Numerical values of parameters used in the L-Q curve

Parameter	TDS	Na^+	K^+	Ca^{2+}	Mg^{2+}	Cl^-	HCO_3^-	SO_4^{2-}
k (m^3/s)	159.000	4.62	1.41	32.100	3.54	3.39	89.000	19.800
γ (m^3/s)	143.025	1266.82	130.15	12.273	281.55	1926.95	9.778	399.555

Note: TDS, total dissolved solids.

4 Discussion

The results until present are summarized in Table 2. The total load from the rivers and groundwater was 47,313,711 tons/a. The dissolved chemical components in the decreasing order were CO_3^{2-}>Cl^->Na^+>Mg^{2+}>HCO_3^- >Ca^{2+}>K^+. As mentioned in the Introduction section, we classified the water quality of salt lakes according to the relationship between Ca^{2+} and HCO_3^-+ CO_3^{2-} in the influent water (Eugster and Hardie, 1978; Mochizuki et al., 2014). Since the water quality composition of Lake Issyk-Kul is of the Na-Cl, SO_4 type, the water quality types of the influent are Ca^{2+}>HCO_3^- +CO_3^{2-}, SO_4^{2-}>Mg^{2+} and Mg^{2+}> Ca^{2+}, which are consistent with the estimation of the loads in the model. The increase in chemical composition per year in this model is 27.2 mg/L for TDS. The TDS in the measured data of the lake water was 27.5 mg/L and the difference was 0.3 mg/L.

Table 2 Influent river and groundwater loads and water balance of Lake Issyk-Kul

Index	Unit	Kadzhi-Say (South)	Cholpon-Ata (North)	Karakol (East)	Lake Issyk-Kul (Estimation)	Lake Issyk-Kul
Drainage area	km^2	6272	3925	5608	-	6236
Precipitation	mm/a	387	424	306	279	280
Evaporation	mm/a	894	749	823	822	814
River water	km^3/a	0.55	0.38	0.41	1.34	1.30
Groundwater	km^3/a	0.82	0.51	0.74	2.07	2.06
r_E=ΣE/ΣP		2.31	1.77	2.69	2.94	2.91
r_G=ΣQ_g/ΣQ_r		1.49	1.35	1.80	1.55	1.59
TDS loads	t/a	18,777,919	11,757,177	16,778,616	47,313,711	-
Na^+ loads	t/a	4,816,807	3,014,545	4,306,999	12,138,351	-
K^+ loads	t/a	151,817	95,060	135,642	382,519	-
Ca^{2+} loads	t/a	332,681	209,352	294,866	836,899	-
Mg^{2+} loads	t/a	821,432	514,186	734,260	2,069,877	-
Cl^- loads	t/a	5,369,811	3,360,571	4,801,622	13,532,004	-
HCO_3^- loads	t/a	764,929	481,996	676,536	1,923,461	-
SO_4^{2-} loads	t/a	6,520,286	4,081,152	5,829,042	16,430,480	-
ΔH	mm/a	218	227	205	107	110
ΔTDS	g/m^3	10.80	6.80	9.70	27.20	27.50
ΔNa^+	g/m^3	2.77	1.73	2.48	6.98	6.62
ΔK^+	g/m^3	0.09	0.05	0.08	0.22	-
ΔCa^{2+}	g/m^3	0.19	0.12	0.17	0.48	–0.24
ΔMg^{2+}	g/m^3	0.47	0.30	0.42	1.19	–0.23
ΔCl^-	g/m^3	3.09	1.93	2.76	7.79	8.08
ΔHCO_3^-	g/m^3	0.44	0.28	0.39	1.11	8.56
ΔSO_4^{2-}	g/m^3	3.75	2.35	3.35	9.45	4.27

Note: Lake Issyk-Kul data adapted from Savvaitova and Petr (1992), Tsigelnaya (1995) and Romanovsky et al. (2013). TDS, total dissolved solids; r_E, adjust fraction of evaporation; r_G, adjust fraction of groundwater; H, water level of the lake. - means no value.

Ca^{2+}, Mg^{2+}, HCO_3^- and SO_4^{2-} are not stable as dissolved substances because they are precipitated as minerals. In fact, there are many rocks on the shore of Lake Issyk-Kul, which look like carbonate precipitates such as beach rocks (Fig. 6). Energy-dispersive X-ray spectroscopy (EDS) measurements of a rock-cut surface are shown in Figure 6. Since Ca^{2+} and Mg^{2+} were detected by EDS measurements, this rock is considered to be a type of evaporate, in which Ca^{2+}, HCO_3^- and Mg^{2+} from the lake water with a granite core precipitated as $CaCO_3$ and $MgCO_3$. Since the annual changes in Ca^{2+} and Mg^{2+} in the lake water are negative, the minimum values of 0.48 mg/L (Ca^{2+}) and 1.19 mg/L (Mg^{2+}) estimated by the present model are considered to be consumed from the lake water as evaporite.

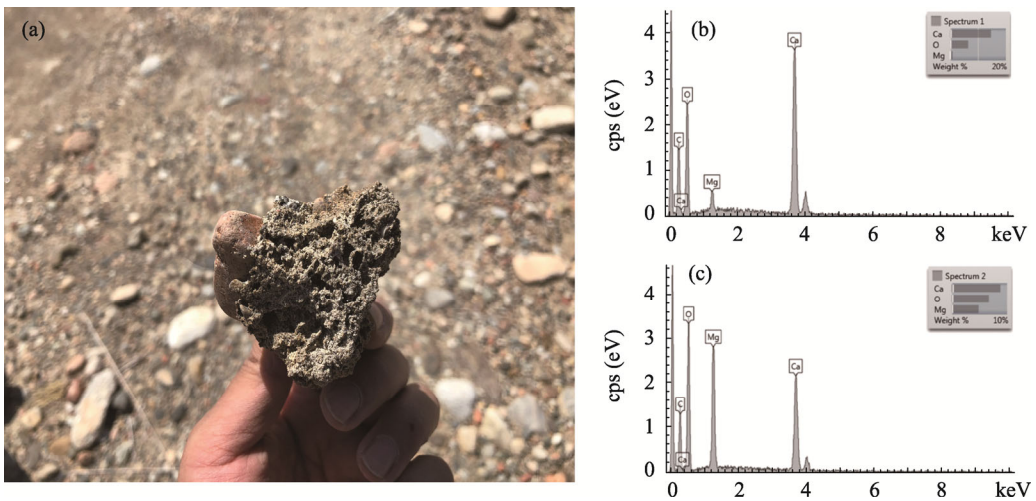

Fig. 6 (a), evaporite found along the southern coast of Lake Issyk-Kul (photo by the author, August 2018); (b and c), energy-dispersive X-ray spectroscopy measurement of a rock-cut surface (courtesy of Dr. Tomokazu HOKADA, National Institute of Polar Research, Japan). In Figure 6b and c, cps (eV) is the counts of eV per second, eV is the energy, and k is the kilo.

Based on the above results, it can be concluded that Lake Issyk-Kul was temporarily desalinated between AD 1500 and 1800 when an outflowing river existed because of the rise in the water level. Thereafter, the outflowing river disappeared as the water level was lowered again, and the chemical components in the inflowing water were concentrated in the lake water. The fact that this lake has full circulation with the mixing of surface and deep water layers throughout the year (Vollmer et al., 2002) suggests that the lake could have discharged enough salt in 300 a. When the lake returned to its blocked state, the inflow water determined the water quality of the lake. Among the components, Ca^{2+}, HCO_3^- and Mg^{2+} were mainly discharged from the lake water as $CaCO_3$ and $MgCO_3$, and the remaining Na^+, Cl^- and SO_4^{2-} increased. The reason for the high Mg^{2+} content in lake water is that the solubility product of $CaCO_3$ and $MgCO_3$ is higher for $MgCO_3$, and hence, Mg^{2+} tends to remain in the lake water. Similar to Mg^{2+}, SO_4^{2-} is also considered to remain in the lake water because its load is higher than its consumption. Further, Na^+ and Cl^- mostly remained in the lake water are the most strongly influenced by groundwater. The influence of groundwater arises from the water inflow from some hot springs (geothermal water) that have higher salinity than the lake (Saitoh, 2019). Kawabata et al. (2014), Saitoh (2019) and Saitoh and Kodera (2019) did not report any simple increasing trend in the change of each chemical component per year, and they found that the salinity repeatedly increased and decreased. These changes occur because the salinity decreases mainly in the surface layer of the lake when water with a low chemical concentration, such as river water and rainfall, enters the lake, and in the long term, the salinity of the lake continues to increase owing to the aforementioned effects. Based on the actual measurement data, in general, the salinity of the lake is expected to increase by 27.5 mg/L yearly unless the lake water is discharged.

5 Conclusions

The results of this study are summarized as follows: the loads from the inflowing groundwater have a high proportion of Na^+ and Cl^- and greatly affect the water quality in Lake Issyk-Kul. In particular, geothermal water has a significant impact on groundwater inflow loads owing to its high concentration of chemical components. Geothermal water is largely responsible for the increased salinity of the lake. Of the Ca^{2+} and Mg^{2+} supplied by river water and groundwater, at least 1.67 mg/L per year is precipitated as $CaCO_3$ and $MgCO_3$, which are widely distributed along the lakeshore as evaporite.

Lake Issyk-Kul was temporarily desalinated during AD 1500–1800 when the outflowing river existed as the water level rose, and then, the outflowing river disappeared as the water level fell again, and the chemical components supplied by the inflowing water were concentrated, resulting in an increase in salinity.

Since river water and precipitation, which do not affect the water quality of the lake, dilute the water quality of the lake and also affect the water level, the salinity of the lake appears to be increasing or decreasing per year. In reality, however, the chemical concentration of the lake water is increasing at a rate of 27.5 mg/L per year. Further, this increase is a natural phenomenon caused by the inflow of groundwater (geothermal water), and hence, the salinity of Lake Issyk-Kul will continue to increase unless the lake water is discharged.

In this study, we assume that Lake Issyk-Kul was a freshwater lake when it was an open lake in the past. However, the water quality of Lake Issyk-Kul is still unclear when it was an open lake. In the future, it is necessary to reconstruct the paleoenvironment of the lake by analyzing diatom taxonomy. In addition, it is necessary to continuously collect basic data such as lake water levels and river flow rates to develop a more accurate water balance model. In this study, we have not been able to analyze the chemical components of the inflow water throughout the year. The challenge will be to improve the accuracy of the inflow water loads by shortening the water sampling intervals and analyzing them in more detail. By clearing these issues, it will be possible to build a more accurate model of the balance of dissolved chemical components. In order to achieve sustainable environmental conservation of saline lakes, it is important to take into account the inflow water loads, which is also important for saline lakes around the world.

Acknowledgements

This study was supported in part by a research grant from the Graduate School of Humanities, Hosei University and Japan Society for the Promotion of Science (JSPS; JP21K13150). We thank Dr. Tomokazu HOKADA of the National Institute of Polar Research (NIPR), Japan, for his assistance in the compositional analysis of evaporites. We are also grateful to Mr. ATANOV Tynchtykbek for his assistance as a field coordinator and guide during the field survey.

References

Alifujiang Y, Abuduwaili J, Groll M, et al. 2021. Changes in intra-annual runoff and its response to climate variability and anthropogenic activity in the Lake Issyk-Kul Basin, Kyrgyzstan. CATENA, 198: 104974, doi: 10.1016/j.catena.2020.104974.

Amano A, Kazama S. 2012. Relationship between discharge and nutrient concentration in inundation areas in Cambodia. Journal of Water & Environment Technology, 10(2): 165–175.

Benduhn F, Renard P. 2019. A dynamic model of the Aral Sea water and salt balance. Journal of Marine Systems, 47(1–4): 35–50.

Chen X, Liu X, Peng W, et al. 2019. Hydroclimatic influence on the salinity and water volume of a plateau lake in southwest China. Science of the Total Environment, 659: 746–755.

Eugster H P, Hardie L A. 1978. Saline lakes. In: Lerman A. Physics. Chemistry: Lakes, Geology. Springer-Verlag: New York, 237–293.

Fukushima Y. 2006. Long-term water level changes in the sky lakes of central Asia Lake Issyk-Kul. Water Science, 49(6): 74–91. (in Japanese)

Gross M. 2017. The world's vanishing lakes. Current Biology, 27(2): R43–R46.

International Lake Environment Committee. 2003. World lake database. [2021-10-22]. https://wldb.ilec.or.jp/Lake/ASI-55.

Karmanchuk A S. 2002. Water chemistry and ecology of Lake Issyk-Kul. In: Klerkx J, Imanackunov B. Lake Issyk-Kul: Its Natural Environment, NATO Science Series (Series IV: Earth and Environmental Sciences). Springer: Dordrecht, 13–26.

Kawabata Y, Kurita T, Nagai M, et al. 2014. Water quality in the Lake Issyk-Kul and the river flowing into it. Journal of Arid Land Studies, 24(1): 105–108.

Korzukhin M D, Kolosov P A, Semenov S M. 2011. Applying Dalton's law of potential evaporation rate over the territory of Russia and neighboring countries using long-term observation data. Russian Meteorology & Hydrology, 36(12): 786–793.

Lensky N G, Dvorkin Y, Lyakhovsky V, et al. 2005. Water, salt, and energy balances of the Dead Sea. Water Resources Research, 41(12): 1–13.

Livingston D A. 1963. Chemical composition of rivers and lakes. In: Nolan T B. Data of Geochemistry (6th ed). Washington: U.S. Government Printing Office, G12–G32.

Meng Q. 2019. Climate change and extreme weather drive the declines of saline lakes: A showcase of the Great Salt Lake. Climate, 7(2): 19.

Miyazako T, Sugahara S, Tabayashi Y, et al. 2014. Comparison of measured and calculated loads using quadratic LQ equation for Hii River flows, eastern Shimane Prefecture, Japan. Japanese Journal of Limnology, 75(3): 151–159. (in Japanese)

Mochizuki A, Murata T, Hosoda K, et al. 2018. Distribution of trace elements and the influence of major ion water chemistry in saline lakes. Limnology and Oceanography, 63(3): 1253–1263.

Narama C. 2012. The natural environment and man in central Eurasia–a millennial history of change and adaptation. In: Narama C. Environmental Change and Humans (Central Eurasian Environmental History). Kyoto: Rinsen Publishing, 288. (in Japanese)

Ricketts R D, Johnson T C, Brown E T, et al. 2001. The Holocene paleolimnology of Lake Issyk-Kul, Kyrgyzstan: trace element and stable isotope composition of ostracodes. Palaeogeography, Palaeoclimatology, Palaeoecology, 176(1–4): 207–227.

Romanovsky V V. 2002. Water level variations and water balance of Lake Issyk-Kul. In: Jean K, Beishen I. Lake Issyk-Kul: Its Natural Environment. Dordrecht: Springer Science+Business Media, 45–57.

Romanovsky V V, Tashbaeva S, Crétaux J F, et al. 2013. The closed Lake Issyk-Kul as an indicator of global warming in Tien Shan. Natural Science, 5(5): 608–623.

Saitoh K. 2019. Geographical study on water chemistry in Lake Issyk-Kul and its catchment, Central Asia. Journal of Geographical Society of Hosei University, 51: 35–44. (in Japanese)

Saitoh K, Kodera K. 2019. Major chemical components of Lake Issyk-Kul and the river and ground water in its catchment area (Central Asia). Journal of Japanese Association of Hydrological Sciences, 49(2): 91–106. (in Japanese)

Salamat A, Abuduwaili J, Shaidyldaeva N. 2015. Impact of climate change on water level fluctuation of Issyk-Kul Lake. Arabian Journal of Geosciences, 8(8): 5361–5371.

Savvaitova K, Petr T. 1992. Lake Issyk-Kul, Kirgizia. International Journal of Salt Lake Research, 1(2): 21–46.

Shope C L, Angeroth C E. 2015. Calculating salt loads to Great Salt Lake and the associated uncertainties for water year 2013; updating a 48 year old standard. Science of the Total Environment, 536: 391–405.

Sugai R, Mizokoyama I, Sugahara S, et al. 2016. Inflow characteristics of pollutant loads from surrounding rivers into Lake Shinji. Japanese Journal of Limnology, 77(2): 117–136. (in Japanese)

Sugawara M. 1972. Outflow Analysis Method (Lectures on Hydrology). Tokyo: Kyoritsu Publishing. (in Japanese)

Tien H Le, Okubo K, Thi P H, et al. 2020. Estimation of long-term external nutrient loading from watersheds to Lake Biwa by a combined rainfall-runoff model and loading-discharge curve approach. Hydrological Research Letters, 14(4): 143–149.

Tsigelnaya D. 1995. Issyk-Kul Lake. In: Maudych A F. Enclosed Seas and Large Lakes of Eastern Europe and Middle Asia, 1. Amsterdam: SPB Academic Publishing, 199–229.

Vollmer M K, Weiss R F, Schlosser P, et al. 2002. Deep-water renewal in Lake Issyk-Kul. Geophysical Research Letters, 29(8): 121–124.

Wurtsbaugh W A, Miller C, Null S E, et al. 2017. Decline of the world's saline lakes. Nature Geoscience, 10(11): 816–821.

Yokota K, Inoue T, Yokokawa M, et al. 2013. Evaluation of the amount of nitrogen and phosphorus runoff load from rivers based on the high-frequency survey. Environmental Science, 26(2): 140–149.

Appendix

Table S1 Date and time of collection and data of for each site

No.	Area (km^2)	Date (yyyy-mm-dd)	Time (LST)	Na^+ (mg/L)	K^+ (mg/L)	Ca^{2+} (mg/L)	Mg^{2+} (mg/L)	Cl^- (mg/L)	HCO_3^- (mg/L)	SO_4^{2-} (mg/L)	NO_3^- (mg/L)	TDS (mg/L)
R1	2.56	2012-08-31	09:53	9.11	1.98	47.9	5.56	4.51	145.0	22.6	1.17	238.0
R2	13.60	2012-08-31	10:12	6.86	2.03	41.3	4.46	4.13	119.0	20.4	-	199.0
R3	10.70	2012-08-31	11:30	1.48	1.07	19.1	1.62	1.02	56.8	4.8	1.88	87.8
R5	49.00	2012-08-31	17:30	3.72	1.22	27.2	2.61	1.98	78.1	12.1	2.19	129.0
R11	59.90	2012-08-31	18:27	4.16	0.84	22.2	2.90	1.71	65.1	14.5	1.40	113.0
R13	1207.00	2012-08-31	19:00	8.87	1.04	53.2	6.17	5.99	153.0	28.5	1.92	259.0
R14	2147.00	2012-08-31	19:30	7.12	1.59	39.4	4.19	4.59	112.0	20.4	2.64	192.0
R16	394.00	2012-09-02	11:55	1.07	0.68	12.6	1.18	1.08	23.4	15.9	1.80	57.7
R17	497.00	2012-09-02	13:20	1.33	0.70	14.9	1.71	1.27	31.8	13.7	1.80	67.1
R18	548.00	2012-09-02	15:50	2.33	0.97	27.0	3.75	1.73	56.1	23.2	1.66	117.0
R19	627.00	2012-09-02	17:10	2.33	1.51	31.9	5.18	1.97	71.0	45.7	2.03	162.0
R21	146.00	2012-09-03	08:45	1.96	0.76	27.1	4.35	1.54	69.3	33.0	1.91	140.0
R23	324.00	2012-09-03	09:10	4.84	1.32	25.2	2.78	3.70	68.3	28.8	1.21	136.0
R24	805.00	2012-09-03	11:45	5.44	1.93	40.2	5.36	3.35	119.0	20.1	2.99	199.0
R27	592.00	2012-09-03	12:45	5.40	1.37	36.4	7.18	4.11	103.0	30.4	-	187.0
R1	2.56	2013-08-24	09:20	8.41	1.76	41.6	5.37	3.91	121.0	32.4	0.65	215.0
R4	31.20	2013-08-26	14:00	4.87	1.47	24.0	2.90	3.45	68.8	18.9	2.41	127.0
R5	49.00	2013-08-26	14:30	2.60	1.16	20.5	1.69	1.38	58.6	11.3	1.90	99.1
R7	371.00	2013-08-26	14:50	2.63	1.11	21.7	1.77	1.37	64.7	11.5	2.15	107.0
R11	59.90	2013-08-26	15:40	3.90	1.29	25.8	3.73	1.52	73.2	26.9	1.15	138.0
G2	-	2013-08-26	16:00	36.40	1.93	43.1	6.38	29.00	127.0	49.2	5.94	299.0
R13	1207.00	2013-08-26	16:30	8.49	1.58	52.9	6.58	6.34	149.0	33.0	1.50	259.0
G4	-	2013-08-26	17:40	48.70	20.30	81.3	41.9	54.4	215.0	180.0	104.00	746.0
R14	2147.00	2013-08-26	19:20	5.32	1.38	34.1	3.85	3.69	101.0	19.4	2.50	172.0
R16	394.00	2013-08-27	12:00	2.15	1.37	25.4	2.71	1.19	75.9	18.7	1.97	129.0
R17	497.00	2013-08-27	12:45	5.83	1.14	28.4	3.45	8.92	82.0	18.2	2.05	150.0
R18	548.00	2013-08-27	13:15	2.78	1.22	29.9	4.05	2.05	83.9	24.8	2.13	151.0
R19	627.00	2013-08-27	13:40	3.19	1.37	39.0	7.18	2.78	90.9	53.3	2.81	201.0
R21	146.00	2013-08-27	15:00	2.53	1.10	19.7	1.90	2.01	59.0	6.1	2.21	94.4
R23	324.00	2013-08-28	09:15	4.86	1.80	26.8	3.23	3.15	76.9	17.2	2.14	136.0
R24	805.00	2013-08-30	07:20	4.35	1.59	33.5	4.84	2.52	92.5	27.1	3.00	170.0
R27	592.00	2013-08-30	08:30	9.40	2.52	59.5	13.3	7.33	175.0	53.2	1.48	321.0
R0	0.78	2014-08-21	10:15	43.30	3.72	117.0	15.5	39.60	322.0	96.5	24.40	661.0
R4	31.20	2014-08-22	10:00	7.96	1.73	35.2	3.02	5.52	102.0	15.7	2.45	173.0
R5	49.00	2014-08-22	10:27	3.10	1.40	28.2	1.72	1.75	78.5	17.7	2.97	135.0
R6	371.00	2014-08-22	10:40	3.72	1.71	28.6	1.80	4.84	76.8	19.5	3.08	140.0
R7	371.00	2014-08-22	11:00	3.67	1.13	28.7	2.31	2.18	80.3	15.1	3.75	137.0
R11	59.90	2014-08-22	11:50	8.89	1.61	49.2	4.86	5.73	142.0	27.0	2.60	242.0
G2		2014-08-22	12:00	38.00	1.72	50.2	5.74	30.20	150.0	37.6	6.09	320.0
R13	1207.00	2014-08-22	12:20	14.10	1.58	61.5	7.24	10.00	168.0	43.1	2.51	308.0
R14	2147.00	2014-08-22	12:55	10.80	1.55	51.5	4.26	6.67	153.0	30.3	3.36	262.0
R16	394.00	2014-08-23	10:15	2.18	1.35	29.5	2.27	1.17	70.4	20.5	2.65	130.0

To be continued

Continued

No.	Area (km^2)	Date (yyyy-mm-dd)	Time (LST)	Na^+ (mg/L)	K^+ (mg/L)	Ca^{2+} (mg/L)	Mg^{2+} (mg/L)	Cl^- (mg/L)	HCO_3^- (mg/L)	SO_4^{2-} (mg/L)	NO_3^- (mg/L)	TDS (mg/L)
R18	548.00	2014-08-24	11:15	3.46	1.44	38.3	3.58	2.67	84.7	31.1	2.62	168.0
R19	627.00	2014-08-24	11:45	4.23	1.65	49.9	6.06	3.83	101.0	54.5	2.10	223.0
R21	146.00	2014-08-24	12:35	3.09	1.09	40.2	5.45	2.14	90.6	42.4	3.36	188.0
R22	145.00	2014-08-24	12:50	4.28	1.81	35.9	3.02	2.69	109.0	9.9	3.30	170.0
R23	324.00	2014-08-24	13:10	9.12	2.26	39.3	3.51	6.72	124.0	11.3	3.51	199.0
R26	725.00	2014-08-24	14:10	13.80	3.93	71.0	12.7	11.20	192.0	58.4	6.56	370.0
R27	592.00	2014-08-24	15:40	9.79	3.59	56.1	8.35	5.59	169.0	32.8	13.80	299.0
R4	31.20	2015-08-22	10:02	4.00	1.70	30.3	4.87	6.14	83.5	16.9	1.99	149.0
R5	49.00	2015-08-22	10:15	3.14	1.27	24.6	3.27	1.01	86.5	5.6	1.80	127.0
R6	371.00	2015-08-22	10:33	4.57	0.95	19.9	2.60	2.19	70.2	6.8	1.82	109.0
R7	371.00	2015-08-22	10:55	3.38	1.52	22.9	2.42	1.85	62.8	16.7	1.82	113.0
R8	231.00	2015-08-22	11:08	2.55	1.21	21.1	1.92	1.78	58.4	14.7	2.08	104.0
R9	111.00	2015-08-22	11:27	3.23	1.14	21.9	2.80	1.42	64.6	13.9	1.91	111.0
R10	97.10	2015-08-22	11:52	1.64	0.51	19.4	2.20	1.86	60.5	9.1	1.76	97.0
R11	59.90	2015-08-22	12:06	3.23	0.84	24.1	3.37	1.72	78.3	11.1	1.37	124.0
G2		2015-08-22	12:36	44.40	2.08	41.3	7.26	15.50	184.0	31.4	5.43	331.0
R12	67.70	2015-08-22	12:46	3.80	0.70	19.5	1.78	2.34	64.5	4.1	1.70	98.3
R13	1207.00	2015-08-22	13:07	13.50	1.66	52.7	7.19	11.20	193.0	37.2	1.08	318.0
R14	2147.00	2015-08-22	14:03	6.69	0.70	33.7	3.45	9.37	99.6	19.5	0.91	174.0
G7		2015-08-23	11:47	24.60	0.23	88.3	13.00	25.80	243.0	57.9	0.00	452.0
G6		2015-08-23	12:00	29.10	0.64	43.5	7.39	23.30	167.0	36.9	5.98	314.0
G3		2015-08-23	14:33	12.60	0.11	40.4	4.32	7.66	119.0	21.8	3.77	210.0
G5		2015-08-23	14:56	151.00	16.60	90.0	24.40	125.00	237.0	227.0	0.00	871.0
G4		2015-08-23	15:20	69.30	10.40	160.0	48.30	91.20	323.0	204.0	201.00	1107.0
R15	138.00	2015-08-23	15:42	13.20	5.14	61.6	10.60	8.22	230.0	34.1	3.59	366.0
G9		2015-08-25	11:11	7.52	1.16	33.4	0.02	4.07	84.3	24.4	2.10	157.0
G8		2015-08-25	11:37	13.00	1.85	71.0	9.51	10.70	277.0	15.8	3.37	402.0
G10		2015-08-25	12:48	4.57	0.59	50.7	3.21	4.10	152.0	10.9	1.17	227.0
G11		2015-08-25	13:14	6.46	1.85	43.0	5.17	2.65	110.0	40.8	1.55	211.0
G12		2015-08-25	13:32	119.00	0.46	16.1	0.50	73.30	94.0	116.0	0.00	420.0
R16	394.00	2015-08-26	09:15	2.39	1.42	14.0	3.05	2.46	32.4	20.9	1.61	783.0
G13		2015-08-26	10:00	3265.00	45.00	1977.0	0.00	7898.00	19.7	723.0	1122.00	15,050.0
R17	497.00	2015-08-26	10:45	7.86	1.38	25.6	4.61	11.50	65.0	20.8	1.21	138.0
R18	548.00	2015-08-26	11:05	2.80	1.19	29.8	4.33	2.66	75.4	28.6	1.72	147.0
G14		2015-08-26	11:35	5.76	1.94	35.3	5.50	5.37	85.1	54.0	2.02	195.0
R20	102.00	2015-08-26	11:56	3.45	0.90	23.3	2.17	4.17	63.9	9.7	1.88	109.0
R21	146.00	2015-08-26	12:07	2.27	1.10	20.7	2.20	1.31	54.6	21.7	1.79	106.0
R22	145.00	2015-08-26	13:18	4.09	1.83	28.8	3.78	4.76	97.5	8.7	2.10	152.0
G15		2015-08-26	13:37	39.50	4.30	84.1	16.00	67.30	253.0	47.2	5.85	517.0
R23	324.00	2015-08-26	13:47	6.19	1.75	27.0	3.66	7.00	91.9	9.7	2.28	150.0
R24	805.00	2015-08-27	09:05	4.80	1.19	22.2	2.87	2.81	73.2	6.0	2.74	116.0
G16		2015-08-27	09:15	50.50	2.20	44.4	6.77	21.00	200.0	37.8	1.56	364.0
R25	805.00	2015-08-27	09:27	7.20	3.31	33.6	5.07	8.40	107.0	22.2	1.74	189.0
R26	725.00	2015-08-27	09:48	8.96	2.87	45.5	9.16	4.51	153.0	30.3	1.70	256.0
R27	592.00	2015-08-27	10:17	12.10	2.02	50.2	15.90	6.55	203.0	49.2	1.12	340.0
G1		2015-08-27	13:18	18.30	0.95	55.6	10.80	12.10	190.0	47.7	2.90	338.0

Table S2 Parameters used in the tank model

Direction	α_{1u}	α_{1l}	α_2	α_3	α_4	β_1	β_2	β_3
North	0.03	0.02	0.03	0.01	0.0000012	0.010	0.020	0.005
East	0.03	0.02	0.03	0.01	0.0000012	0.030	0.020	0.010
South	0.03	0.02	0.03	0.01	0.0000012	0.010	0.020	0.001

Note: α_i and β_i are the constants that specify runoff and infiltration rates proportional to the relative height to the runoff outlet and the tank depth, respectively.